Pressure-induced phase transition of nanocrystalline ZnSe

2005 J. Phys.: Condens. Matter 17 5187

(http://iopscience.iop.org/0953-8984/17/34/003)

INSTITUTE OF PHYSICS PUBLISHING JOURNAL OF PHYSICS: CONDENSED MATTER

J. Phys.: Condens. Matter **17** (2005) 5187–5200 doi:10.1088/0953-8984/17/34/003

Pressure-induced phase transition of nanocrystalline ZnSe

C E M Campos[1], J C de Lima[1], T A Grandi[1], J P Itié[2], A Polian[2] and A Michalowicz[3]

[1] Departamento de Física, Universidade Federal de Santa Catarina, C.P. 476, 88 040-900 Florianópolis, SC, Brazil
[2] Laboratoire de Physique des Milieux Condensés, Université Pierre et Marie Curie, Campus Boucicaut, 75015 Paris, France
[3] Groupe de Physique Structurale des Molécules et Matériaux, Université Paris XII Val de Marne, 94010 Créteil, France

E-mail: pcemc@fisica.ufsc.br

Received 14 March 2005, in final form 21 June 2005
Published 12 August 2005
Online at stacks.iop.org/JPhysCM/17/5187

Abstract

X-ray absorption spectroscopy and Raman experiments were used to follow the semiconductor–metal phase transition of nanocrystalline ZnSe produced by mechanical alloying. The results were used to compare the physical properties of nanometric crystals with those of the standard bulk ones. Due to the crystal size reduction, we observed an increase of the phase-transition pressure. The structural evolution of non-reacted Se with pressure was observed by Raman spectroscopy. This fraction of Se was found to be nanostructured. Thermal annealing showed itself to be an efficient way to manipulate this Se balance, as well as to recover the crystallinity of ZnSe phase.

1. Introduction

Zinc selenide is a semiconductor material at ambient conditions of technological importance for use as an infrared filter or lenses, or for short wavelength visible light laser devices [1]. For this last application, it has been shown that the materials should be of nanometric size, with grains smaller that the ZnSe Bohr exciton diameter (∼90 Å).

Nanometre-sized crystalline materials are polycrystals in which the size of individual crystallites is of the order of several (1–10) nanometres [2]. These materials are composed of the following two components: a crystalline component formed by all atoms located in the lattice of the crystallites (grains) and an interfacial component comprising all atoms situated in the grain boundaries (or interphase) between the crystallites. Moreover, the number of atoms in each component is comparable. The atomic structure of the interface is known to depend on the orientation of the relationship between the adjacent crystallites and the boundary inclination. If the crystallites are oriented randomly, all of the grain boundaries of a nanometre-sized crystalline material have different interatomic spacings. According to Gleiter [2] a

nanometre-sized crystalline material with a crystallite size of 5 nm contains typically about 10^{19} interfaces cm^{-3}. Then, the interfacial component structure is the sum of the 10^{19} interfacial structures. If the interatomic spacings in all boundaries are different, the average of 10^{19} different boundaries results in no preferred interatomic spacing, except those prevented by interatomic penetration. Hence, the interfacial component is interpreted as a solid-state structure without long- or short-range order [3], which can be manipulated to reach new technological applications even for well-known materials.

The simple polymorphism of bulk ZnSe when submitted to high-pressure and/or high-temperature conditions makes it a model compound which has attracted considerable attention. At room temperature it transforms from a zinc-blende (ZB) to rocksalt (RS) structure at 13.5 GPa [4]. This transformation is associated with a semiconductor–metal transition. From a local point of view, the principal effect is the coordination number increase. Recently, theoretical calculations [5, 6] reported the existence of two intermediate phases (cinnabar and simple cubic 16) in the 9–13.4 GPa range, but only the cinnabar one was observed experimentally at temperatures below 300 °C [7, 8].

ZnSe prepared by mechanical grinding (MG) has been studied by energy dispersive x-ray diffraction (EDXD) and Raman spectroscopy up 120 and 11 GPa, respectively [9]. In that paper the authors reported a structural evolution sequence ZB–RS–SH (simple hexagonal) as a function of pressure and pointed out some anomalies in the equation of states and Raman measurements at 5 GPa. A mixture of ZB and RS was detected between 11.8 and 14.5 GPa, and above 16.9 GPa only RS was observed. Between 12 and 47 GPa a disturbed RS was indexed, while for 47 GPa a perfect RS phase was proposed. At 48 GPa a simple hexagonal (SH) phase was observed with a special particularity: there was a diffraction peak (called the '*d*' line) which has been associated to a defect feature, such as an important number of lattice vacancies.

More recently, we have shown that nanometric ZnSe polycrystals with the ZB structure can be synthesized by mechanical alloying (MA) starting from elemental powder mixtures Zn_xSe_{1-x} [10, 11]; however, in all concentrations x studied non-reacted elements were detected, even in the stoichiometric mixture ($x = 0.5$). Moreover, ageing effects—consisting basically of segregation of Se particles—and the hydrophilic character of the samples were reported. These samples will be cited as MA-ZnSe and aged-MA-ZnSe in the following. It is important to emphasize here that the MA method starts from a mixture of elemental Zn and Se powders to obtain a nanometric alloy, while the MG process starts from a ZnSe compound. In a previous paper, vibrational profiles of the optical phonons of both aged- and MA-ZnSe samples were traced [12]. They showed the Se_n chain modes and TO- and LO-ZnSe modes. The most important changes in the Raman parameters of these phonons with ageing were associated with growing of Se phase and with rising of stress conditions and reduction of bond effective-charge of the ZnSe phase. Furthermore, thermal treatments of the aged-MA-ZnSe sample implied an important crystallinity recovering of the ZnSe phase and a partial separation of the non-reacted Se at temperatures much smaller than its boiling point.

The goal of the present paper is to follow the semiconductor–metal phase transition of nanocrystalline ZnSe produced by MA (MA-ZnSe) using x-ray absorption spectroscopy (XAS) and Raman experiments, and to compare some physical properties of the nanocrystals with those of the standard bulk ones.

2. Experimental details

The $Zn_{50}Se_{50}$ sample was prepared by MA after 50 h of milling using a ball-to-powder ratio of 2.6 (this sample will be called MA-ZnSe) [10]. The pattern of the MA-ZnSe sample showed a ZnSe phase that was indexed as a zinc-blende structure with space group $F\bar{3}m$ and lattice

parameter 5.6478 Å (refined by the Rietveld method [13]). A small portion of the MA sample was submitted to a quenching process from 350 °C, followed by slow annealing at 500 °C (this sample will be called ta-MA-ZnSe). From this procedure, a phase separation was observed in the quartz tube: part of the sample remain deposited in the inner walls of the tube after annealing, and the major part was collected and analysed by XRD and DSC techniques. The results showed that both MA-ZnSe and annealed samples have the same crystalline phases and there is practically no Se excess in the ta-MA-ZnSe, which was sublimed and deposited in the quartz tube. The mean crystallite size for the ZnSe phase was calculated using the Scherrer formula [14] and the values obtained were ∼10 nm for MA-ZnSe and ∼20 nm for ta-MA-ZnSe. More details about the sample preparation and their structural, thermal and optical characterizations can be found in our previous studies [10–12]. Chemical analyses of the samples were performed by x-ray fluorescence (EDX) and the values obtained were 41.9 at.% Zn, 40.3 at.% Se and 17.8 at.% O for MA-ZnSe 54.6 at.% Zn, 34.7 at.% Se and 10.7 at.% O for ta-MA-ZnSe.

A diamond anvil cell (DAC) was used as the pressure inductor up to 31.5 GPa. A methanol/ethanol/water mixture (16:3:1) and neon gas were used as the pressure transmitting medium in absorption and Raman experiments, respectively. The pressure determination during both experiments was performed through the pressure-dependent fluorescence of a ruby chip.

Absorption experiments were performed at the Zn K-edge (9.659 keV) at D11 dispersive station in Laboratoire pour l'Utilisation du Rayonnement Electromagnétique (LURE), Orsay, France. EXAFS analysis was carried out by using the program set written by Michalowicz [15], according to the recommended procedures described by the Standards and Criteria in XAFS Committee of the International XAFS Society [16].

XAS is a very well adapted technique to study pressure-induced coordination changes in zinc-blende-type semiconductors, associated to a transition to a metallic state. The study of phase transformations following the short-distance order modifications, as given by XAS, has several advantages over the studies of long-distance order obtained by diffraction experiments. The main advantage is that it directly provides the coordination numbers and interatomic distances around a selected absorbing atom. Furthermore, studies following the evolution of the disorder parameter (Debye–Waller) as a function of pressure can probe more accurately the exact pressure for which the phase transition starts. Moreover, when both phases are present, the spectra correspond to a weighted sum of low- and high-pressure phase spectra (as will show in figure 2 in next section).

Raman scattering measurements were performed at ambient temperature in an XY Dilor monochromator, in the subtractive mode, coupled to an optical focal lens (20×) and CCD detecting system. This set-up give an uncertainty of about 2 cm^{-1} in the Raman line peak position. The 514.5 nm line of an argon ion laser was used as exciting light always in backscattering geometry, and an output power below 5 mW was used to avoid any overheating of the sample.

3. Results and discussions

3.1. X-ray absorption measurements

Figure 1 shows the absorption spectra of the MA-ZnSe sample as a function of pressure (up 25 GPa) and at ambient temperature. Several modifications take place in the spectra as the pressure increases. This figure also shows the spectrum collected after pressure relaxation (see dotted line). Considering the reasonable similarities between the spectra before and after the pressure testing, one can conclude that the phase transition is reversible.

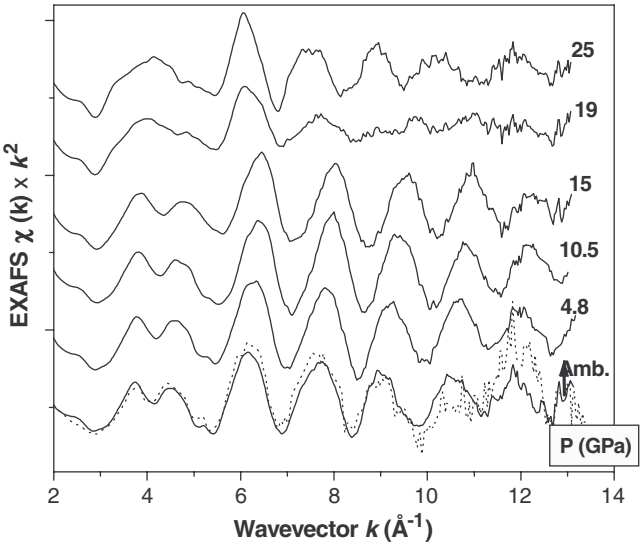

Figure 1. EXAFS spectra of MA-ZnSe sample as a function of pressure. The dotted line represents the spectrum collected after pressure relaxation.

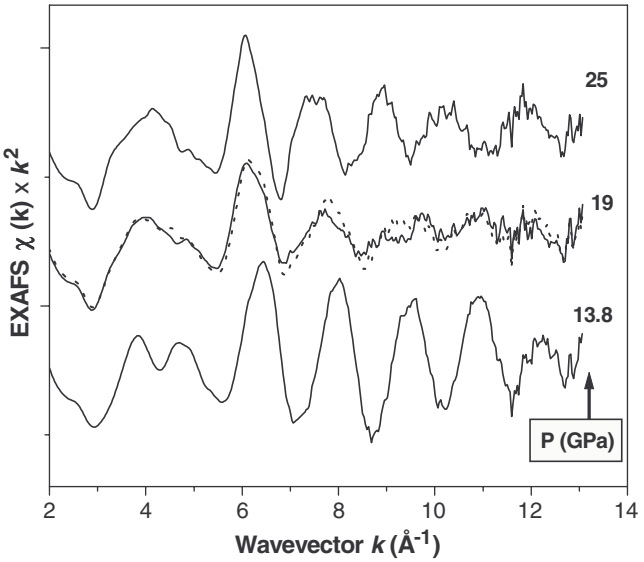

Figure 2. Weighted averaging of EXAFS spectra of MA-ZnSe sample. The dotted line represents the best simulation of the spectrum at 19 GPa reached using 45% of the spectrum at 13.8 GPa and 55% of that at 25 GPa.

At ambient conditions, the x-ray absorption near-edge structure (XANES) region showed a white line and a multipeak pattern, commonly observed for several systems that have a tetrahedral configuration around Zn atom, such as ZnTe [17] and ZnS [18]. All these XANES features shifted to higher energies as the pressure increased up to 10.5 GPa. This XANES features behaviour has also been observed in multiple-scattering calculations of ZnS [18] when decreasing the distance between atoms. This is also the common observed behaviour in other isotropically compressible materials like GaAs [19], GaP [20] and GaN [21]. For pressures higher than 15 GPa a dramatic change in XANES is accompanied by rise in the first-neighbour distance (see figure 5(b)). Considering the XANES sensitivity to the local coordination, interatomic distances, electronic configuration, and based in the theoretical calculations of ZnS (which have shown that to reproduce the Zn K-edge XANES it is necessary to consider neighbour shells around the absorber up to the fifth shell), one can conclude that

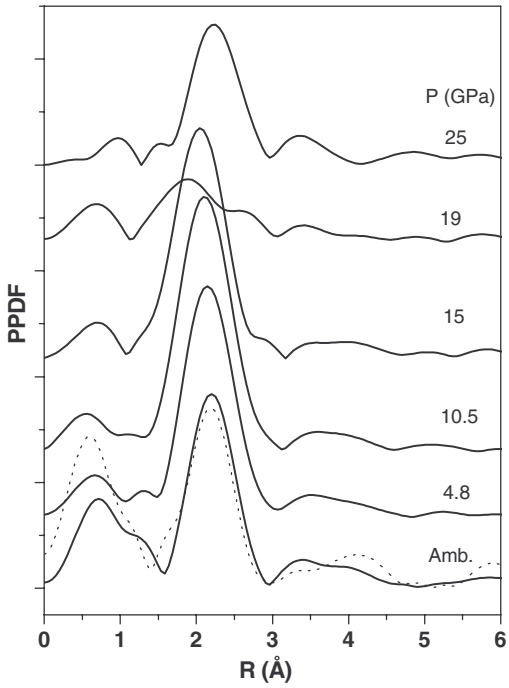

Figure 3. Fourier transform functions of MA-ZnSe sample as a function of pressure. The dotted line represents the spectrum collected after pressure relaxation.

a drastic change in XANES is evidence of a transition to a new phase with increase of the coordination number.

The EXAFS oscillations showed important modifications with pressure increasing, especially at 19 GPa when some oscillations disappeared (see figure 1), indicating destructive interferences probably due to the coexistence of ZB and RS phases. It is interesting to note that for the highest pressure tested (25 GPa) the spectrum is completely different from that obtained at ambient pressure. The coexistence of ZB and RS phases was proposed to exist between 17 and 23.3 GPa. The contribution of each phase was estimated by weighted averaging the spectra at 13.8 and 25 GPa. Figure 2 shows that the spectrum at 19 GPa represents a mixture of 45% ZB and 55% RS. It is interesting to observe that the pressure domain where the phase transition occurs for MA-ZnSe sample is at least 1 GPa higher than those reported for bulk and mechanical ground ZnSe samples.

The EXAFS data extraction was done as follows. First, background corrections were performed to obtain the μ_0 contribution. The edge position was defined by the second derivate method and a range definition was made: the first 50 eV of the spectra (XANES region) were ignored. Moreover, the spectra were converted to reciprocal space, from energy to wavevector (k). Then, Fourier transforming operations generated the pair-pseudo-distribution functions (PPDFs) using Kaiser apodization windows (with $\tau = 2.5$) and third-order terms in k (between 3.4 and 13.3 Å^{-1}).

Figure 3 shows the evolution of the PPDF as a function of the pressure. It can be seen that the contribution of the first coordination shell to the EXAFS PPDF gradually shifts its position to smaller distances in the pressure domain between ambient pressure and 15 GPa, and the intensity grows as expected from the decrease of the dynamical disorder, as will be discussed later. For pressures higher than 15 GPa a rise in the first-neighbour distance of about 0.1 Å (figure 5(b)) is accompanied by a dramatic change in the XANES. A large increase in the relative Debye–Waller factor was also seen (figure 5(a)), which is only interpretable as a

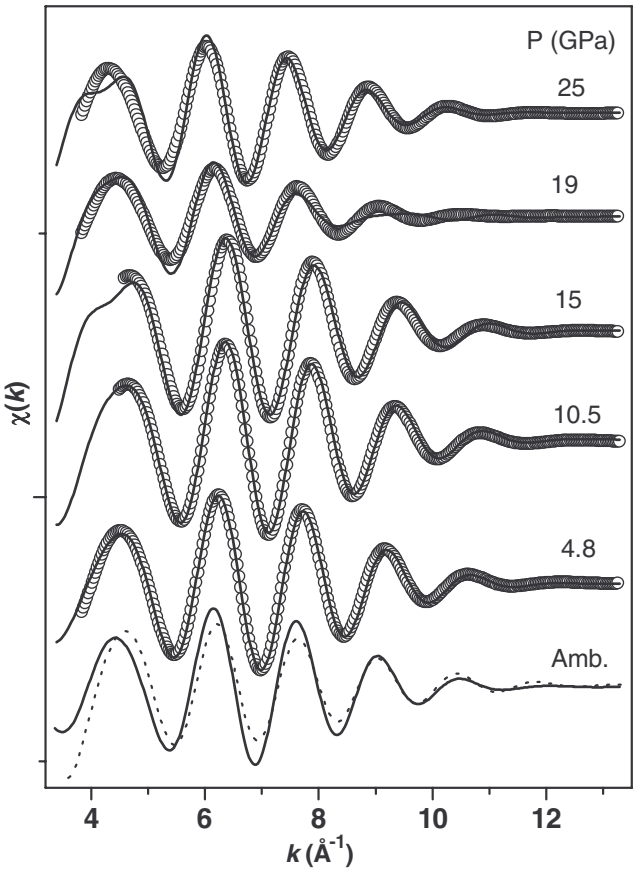

Figure 4. Experimental (lines) and simulated (symbols) EXAFS signals of MA-ZnSe as a function of pressure. The dotted line represents the spectrum collected after pressure relaxation.

consequence of the apparition of static disorder coming from a phase mixture. The PPDF after pressure relaxation shows the main peak position slightly downshifted and important changes in the relative intensities of the second band (3–4.5 Å) if compared with the PPDF observed before the pressure test. It is interesting to note that the sample returned to the initial structure at ambient, showing no sign of amorphization, but the edge drops drastically to a value ∼2 eV lower as compared with the initial spectra at ambient conditions (see dashed line in the inset of the XANES region in figure 1). Although the literature affirms that in ZnS and ZnSe the reverse transition between the RS and ZB phase takes place without hysteresis [17], these facts strengthen the hypothesis of pressure-induced hysteresis effects in the MA-ZnSe. However, some problems concerning this analysis can be pointed out, such as the spurious harmonics that could have been a source of contamination of the x-ray beam, and the effects of nonlinearity of the detector response to the photon flux may also be responsible for the observation of false hysteresis effects.

The inverse-FT functions, i.e. the EXAFS signals $\chi(k)$, were extracted from the 1.2 and 3.1 Å region of the PPDFs, which represents the first coordination sphere. Figure 4 shows the EXAFS signals for the MA-ZnSe sample as a function of pressure. Simulated EXAFS signals were proposed for experimental signals collected at higher pressures (see the symbols in figure 4). From these simulations the evolution of average distance (d) of Zn nearest-neighbours and the relative Debye–Waller ($\Delta\sigma^2$) parameter as a function of the pressure were determined, and these are presented in figure 5. For that the total

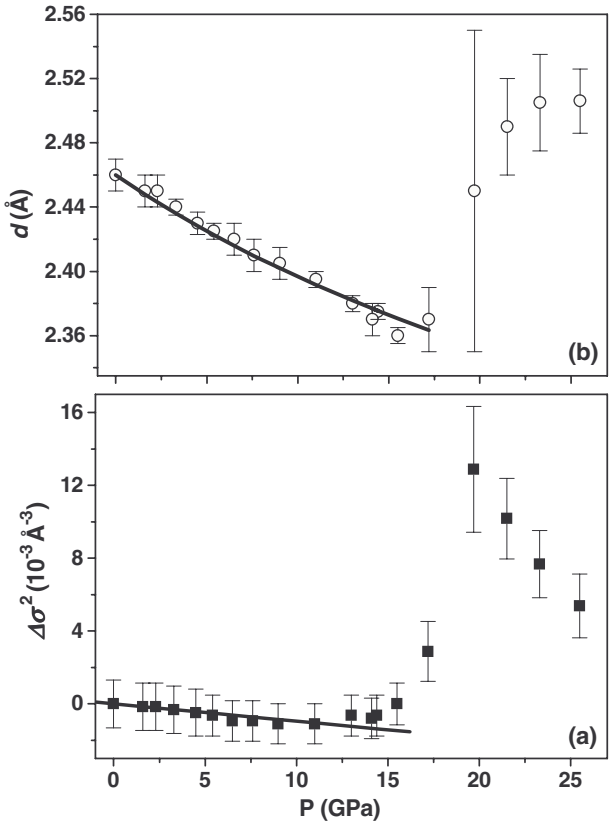

Figure 5. Relative Debye–Waller factor (a) and Zn nearest-neighbour distances (b) of MA-ZnSe sample as a function of pressure. Solid lines represent the dynamic part of relative Debye–Waller factor calculated according to the Einstein model (a) and the best fitting achieved using the Murnaghan equation (b).

phase shift and backscattering amplitude were extracted from FEFF calculations obtained for pair distances Zn–Se smaller than 2.6 Å, which considering the short-range crystallographic information for the ZB phase [22][4] (coordination number $N = 4$ and first-neighbour distance $d = 2.454$ Å). The changes in the coordination number (N) and relative Debye–Waller ($\Delta\sigma^2$) parameter are strongly correlated, and then the fitting procedure was performed fixing N and electronic parameters (since electronic functions—electron mean free path, total phase shift and backscattering amplitude—are considered pressure independents). However, it is interesting to mention that for pressures higher than 20 GPa several tests were done considering $N = 4$ or 6, and the fittings using the higher coordination number furnished better quality factors. The experimental statistical errors, the quality of the fits and the error bars on the fitted parameters were evaluated with the standard procedures recommended by the IXS Standards and Criteria Committee [15]. The results reported in figure 5 strongly evidence a phase transition from fourfold to sixfold coordination, with a corresponding increase of the Zn–Se distance from 2.36 to 2.50 Å. It is interesting to mention that all the spectra were fitted with a satisfying quality factor (QF $\leqslant$ 1) using one single shell, except the one collected at 19 GPa, which required three shells, with an average distance 2.45 Å. This difficulty is reported in figure 5(b) by the large average distance error bar at this pressure.

Figure 5(a) shows the relative Debye–Waller ($\Delta\sigma^2$) parameter as a function of pressure for the MA-ZnSe sample. For pressures smaller than 15 GPa an important reduction of $\Delta\sigma^2$ parameter was observed, that can be explained as a decreasing of dynamical disorder. On

[4] Atomic Softek, 70 Longwood Road North, Hamilton, Ontario, L8S 3V4, Canada.

continuing the compression from 15 GPa up to ∼20 GPa, the $\Delta\sigma^2$ parameter increased, and this could be only interpretable as a consequence of the apparition of static disorder coming from the phase mixture (ZB and RS). In the higher pressure domain studied (20–25 GPa) the $\Delta\sigma^2$ parameter decreases. In a first view, this is interpreted as the disappearance of the static disorder, a consequence of the stabilization of the RS phase. In a second view, this evolution represents the decrease of dynamic disorder from the compression of RS phase that continues up to 25 GPa. In the pressure domain from 15 to 25 GPa a shift of the edge position towards lower energies of about 0.2 eV is observed. This is an expected feature from the metallization (semiconductor–metal transition), which is associated with a large change in the band structure. From this observation one can conclude that there is an increasing of at least 1 GPa in the pressure where the ZB–RS phase transition occurs for MA-ZnSe as compared with values reported for both bulk and mechanical ground ZnSe [7, 9]. However, several problems can be pointed out about this conclusion, such as the existence of important amounts of O and Se nanocrystals (as will be shown in section 3.2) in the sample. On the other hand, it is important to compare the properties of a sample produced by MA with those prepared by other methods. Moreover, the accuracy in the observed $\Delta\sigma^2$ is quite limited, mainly due to the spectra normalization procedure. It is affected by the presence of diffraction glitches, which limit the extent of the usable energy domain above and below the edge.

It is possible to combine the Einstein approximation with Raman scattering data under pressure to evaluate in a first-order approximation the evolution of the harmonic dynamic part of σ^2 [23]. If the Grüneisen parameter for the LO mode is known, the expected pressure dependence of the harmonic dynamic part of σ^2 can be related to the first-neighbour distance variation by

$$\frac{\Delta\sigma^2}{\sigma^2} = 6\gamma_{\mathrm{LO}}\frac{\Delta d}{d} \tag{1}$$

where $\gamma_{\mathrm{LO}} = \mathrm{d}\ln\omega_{\mathrm{LO}}/\mathrm{d}\ln P$ is the Grüneisen parameter. For MA-ZnSe $\omega_{\mathrm{LO}} = 250\ \mathrm{cm}^{-1}$ and $\mathrm{d}\omega_{\mathrm{LO}}/\mathrm{d}P = 3.57\ \mathrm{cm}^{-1}\ \mathrm{GPa}^{-1}$ from Raman measurements (see section 3.2). So the expected dependence of $\Delta\sigma^2$ with pressure for an isotropic compression in an Einstein model is $0.9 \times 10^{-4}\ \text{Å}^2\ \mathrm{GPa}^{-1}$. This angular coefficient was then used to plot theoretical $\Delta\sigma^2$ evolution with pressure in figure 5(a), viewing a simple comparison with the experimental results.

Figure 5(b) shows the interatomic distance (d) evolution with pressure for MA-ZnSe. A reduction of about 3.5% in the nearest-neighbour distance was observed when the pressure reached 15 GPa. As the computation of the molar volume variation with pressure (equation of state) is one of the most stringent test for (in)validation of models and theories, the interatomic distance data with pressure, $d(P)$, were fitted by a first-order Murnaghan's state equation [24]. From this procedure the inverse linear compressibility (B_{Lo}) and its derivate in relation to pressure (B'_L) were determined.

$$d(P) = d_0\left(1 + \frac{B'_{\mathrm{L}} \cdot P}{B_{\mathrm{Lo}}}\right)^{\frac{-1}{3B'_{\mathrm{L}}}}. \tag{2}$$

The values obtained were $B_{\mathrm{Lo}} = 104.5$ GPa and $B'_L = 5.0$ for the ZB phase of the MA-ZnSe sample. Unfortunately, the data concerning the RS phase were insufficient to determine their B_{Lo} and B'_L values. A large number of experimental studies that furnish bulk modulus (B_0) values for bulk ZnSe have been reported in the literature. In these papers there are B_0 values from 39 to about 70 GPa; some of them have furnished derivate (B'_0) values that vary from 4 to 5 [4, 8, 9, 25]. In some theoretical studies B_0 has been predicted to be as high as 75 GPa [26], but more recent calculations have shown $B_0 = 65.7$ GPa [27], in better agreement

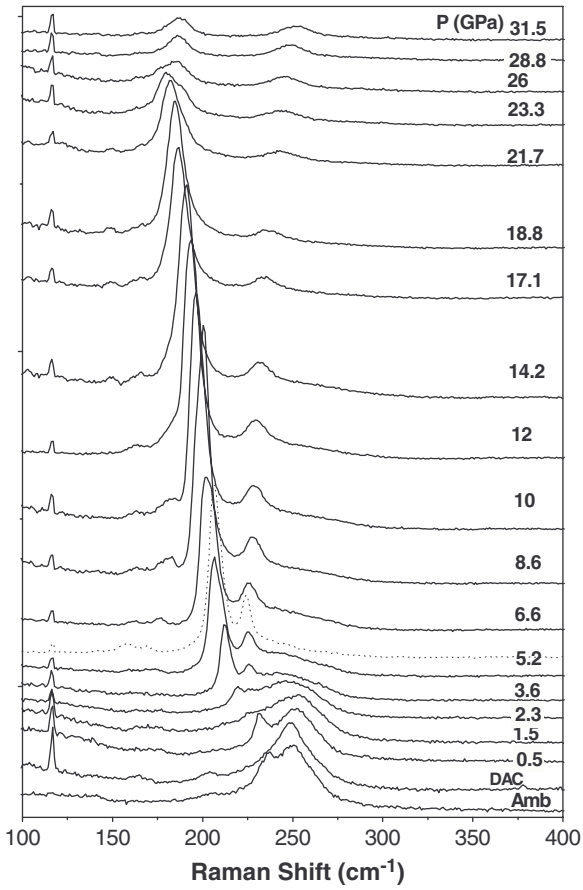

Figure 6. Raman spectra of the MA-ZnSe sample as a function of pressure. The dotted line represents the spectrum collected after pressure relaxation.

with experimental results. It is interesting to note that the values obtained for MA-ZnSe sample are even greater than those reported for the mechanically ground sample ($B_0 = 67$ GPa and $B_0' = 4.2$). This fact suggests that the small particle size of the MA-ZnSe can be responsible for the high B_{Lo} value observed, indicating that nanoparticles are less compressible than bulk ones. Although contamination of mechanically alloyed powder still figures as the biggest problem to corroborate this interpretation. Moreover, other problems can be responsible for the large values found in this paper, such as the non-transferability of the EXAFS phase-shift function due to electronic changes or to decrease of distances with pressure, pressure gradient effects into the gasket hole, etc.

3.2. Raman measurements

Figure 6 shows the Raman spectra of the MA-ZnSe sample as a function of pressure. The triangular line located at about 116 cm^{-1} is a plasma line of the laser. At ambient conditions there are an intense wide band centred at about 250 cm^{-1} and two other weak signals located at approximately 140 and 200 cm^{-1}. As already reported in a previous paper [12], the features at about 250 and 200 cm^{-1} are associated with the LO- and TO-ZnSe modes, respectively. The other two features, at 140 cm^{-1} (E' mode) and 237 cm^{-1} ($A1$ mode), are associated with a small portion of non-reacted Se. The E' and $A1$ modes are produced by the rotational motion about axes perpendicular to the helical axis and helical chain-expansion type vibrations,

respectively. This figure also shows the spectrum collected after partial pressure relaxation (at 5 GPa, see dotted line). Considering that the spectra before and after the pressure testing have the same features, one can conclude that the phase transitions observed by Raman scattering are reversible. It is worth stressing that the Raman measurements of MA-ZnSe are complementary to the XAS ones, since Raman spectroscopy is very sensitive to the non-reacted Se found in this sample. Because of this the pressure ranges where the XAS and Raman data show major changes do not seem to correspond. The Raman measurements were repeated from different portions of the MA-ZnSe sample and the results were well reproduced.

Considering that there is non-reacted Se in the MA-ZnSe it is interesting to review some properties of this element with pressure. Bulk Se is known to have five pressure-induced phase transitions. The transformation sequence with increasing pressure is hexagonal → monoclinic(I) → monoclinic(II) → orthorhombic → rhombohedral and cubic at 14, 23, 28, 60 and 140 GPa, respectively [28, 29]. In the more recent paper [29], reporting energy dispersive and Raman experiments, the pressure-induced structural transitions of Se in nanocrystalline form (up to 30 GPa) showed a more complex phase transition behaviour with lower transitions pressures and lower symmetry of high-pressure phases as compared to bulk Se. Following this pressure-induced phase transition scene, the high-pressure Raman measurements of the MA-ZnSe sample can determine the structure and dimensional scale (average particle size) of non-reacted Se in the sample.

The first spectrum, at the bottom of figure 6, was collected out of the DAC and, curiously, it was not well reproduced when the sample was introduced in the cell without a pressure transmission medium. Fortunately, after the neon charging (see the spectrum at 0.5 GPa) the Raman profiles of the sample were recovered. Then, nothing surprising was found—the TO and LO modes corresponding to the ZB phase of ZnSe were observed—except for the slight intensity increase of the $A1$ mode (now located at about 230 cm^{-1}).

With pressure increasing the $A1$ mode shifts to lower frequency, indicating a pressure-induced strengthening of the interchain bonds and a weakening of the intrachain ones. This behaviour is responsible for the huge intensity increase of the $A1$ mode with pressure, in agreement with previous reports for bulk and nanocrystalline Se [28, 29]. The strange change of the $A1$ mode at about 14.2 GPa suggests a phase transition, which was identified as an intermediate phase Se(III) observed only in the nanocrystalline form [29]. The $A1$ mode continues the softening trend, and starts to disappear at 23.3 GPa, indicating a structural distortion from the helical-chain microstructure to a denser-packed layer type microstructure (as will be discussed later). This interpretation was made based on energy dispersive x-ray diffraction (EDXD) and Raman studies of nc-Se (nanocrystalline Se) [29], which showed that for pressures higher than 17.5 GPa the chain-like microstructure completely disjoints.

The peaks of the E'' (due to asymmetric breathing motions) and $A1$ modes of Se chains overlap at ambient pressures, and then split with increasing pressure. A phase transition is evidenced at about 5 GPa where the E'' mode has a minimum, and one of the low-frequency weak peaks was upshifted as a function of pressure (see figure 7). Above 23.3 GPa, the weak broad band (where the E'' peak was located) moves from 240 to 250 cm^{-1}. Considering that a structural change from the helical-chain microstructure to a denser-packed layer type one has been observed at about the same pressure [29], the band at 250 cm^{-1} can be associated to the $A1$ mode of the Se_8 rings type microstructure. Moreover, the appearance of a weak band at 120 cm^{-1} in the spectrum at 23.3 GPa suggests a intermediate phase transition to a lower symmetry nc-Se(IV) [29, 30]. These observations corroborate the pressure-induced phase transition scene reported for the nc-Se phase by means of EDXD measurements [29].

Considering that neither crystalline nor amorphous Se were clearly observed by DSC and XRD measurements of this sample [11], the most probable explanation is that there

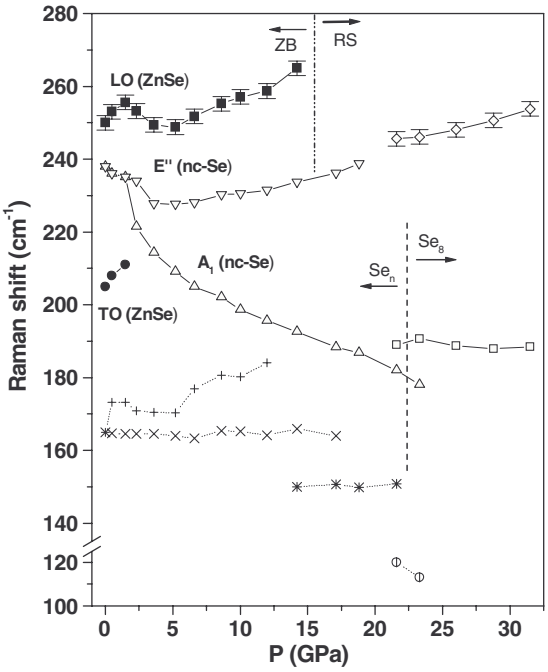

Figure 7. Raman frequency of nc-ZnSe (full symbols) and nc-Se (empty symbols) modes of the MA-ZnSe sample as a function of pressure. Representative error bars are showed for two Raman lines.

was an important amount of Se nanocrystals well dispersed in the interfacial region of the ZnSe crystallites and during the Raman experiments the laser power could be responsible by photo-induced nc-Se nucleation/agglomeration from Se atoms dispersed in the interfacial region. These interpretations are in agreement with the well known characteristic of nanomaterials determined by total structural factors (TSF) analyses of as-milled and post-annealed samples [31]. The TSF analyses have shown that in the as-milled mixture the number of atoms in both components (interfacial and nanocrystallites) is similar.

With increasing pressure the identification of both LO- and TO-ZnSe modes was perturbed due to the interferences of Se modes. However, the pressure-induced dispersion curve of LO-ZnSe was tentatively proposed. From this curve (and from figure 6) one can conclude that the ZB–RS phase transition took place for pressures higher than 14.1 GPa. This observation agrees quite well with the XAS results. Unfortunately, no conclusion could be made about the TO-ZnSe mode, which was completely covered up by Se modes. Figure 7 shows the pressure-induced phonon dispersion curves of the most intense Raman lines of the as-milled sample as a function of pressure. A tentative fitting was done for the first points of LO mode using a linear function. The value obtained was 3.57 cm^{-1} GPa^{-1}. This figure represents the whole pressure-induced phase transition scene of both nanocrystalline ZnSe and Se found in the MA-ZnSe sample.

In order to clarify the existence of non-reacted Se in nanocrystalline form, Raman measurements of the thermally annealed MA-ZnSe (ta-MA-ZnSe) sample were performed. This sample was chose because its ZB phase has a better crystallinity (as compared to the as-milled sample) and a large part of the non-reacted Se was eliminated, there being just a residual Se portion in a special amorphous state (containing mainly Se_8 rings), due to thermal treatments [11]. Figure 8 shows the Raman spectra of the annealed sample as a function of pressure. At ambient conditions almost the same features were observed as for the as-milled sample. The most notable differences observed after annealing are the enormous intensity

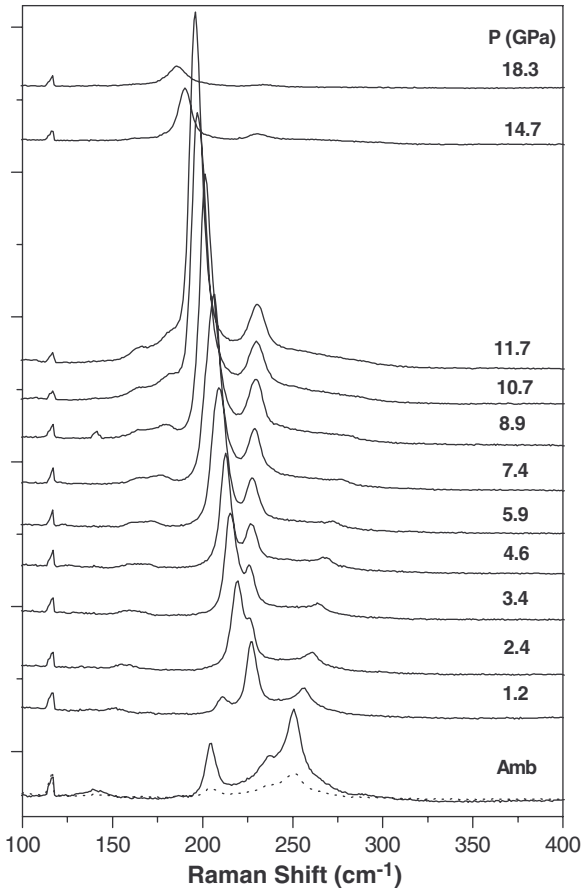

Figure 8. Raman spectra of thermally annealed sample (ta-MA-ZnSe) as a function of pressure. The dotted line represents the spectrum collected after pressure relaxation.

increase of the TO-ZnSe mode and the recovery of the bulk-like parameters for all Raman lines. Moreover, with increasing pressure the LO-ZnSe mode showed more dispersive behaviour as compared with that of the as-milled sample, while the description of the TO mode remains a difficult task. The parameters of the ZB–RS phase transition were also modified, now occurring for pressures between 11.7 and 14.7 GPa, in accordance with the LO disappearing. On the other hand, the Se modes of the annealed sample showed a different behaviour with increasing pressure, as compared to those of as-milled sample, which is very similar to that reported for bulk Se [28].

Figure 9 shows the pressure-induced phonon dispersion curves of the most intense Raman lines of the annealed sample as a function of pressure. Although the $A1$ mode shows the same pressure-induced changes—intensity increasing followed by peak splitting and frequency downshift—for higher pressures (>15 GPa) this peak completely disappears. Furthermore, at the same pressures all other lines also abruptly disappeared, there remaining just a weak and large peak at about 180 cm^{-1}. The LO-ZnSe mode dispersion was quantified by means of a second-order polynomial fitting and the values obtained (4.30 cm^{-1} GPa^{-1} and -0.12 cm^{-1} GPa^{-2}) were slightly smaller than those reported for a bulk sample [9]. In that paper [9] the authors reported a discontinuity of TO- and LO-ZnSe modes at about 5 GPa, which was attributed to the sample preparation process (mechanical grinding). It is interesting to note that, even though the synthesis method used in this study is also based on

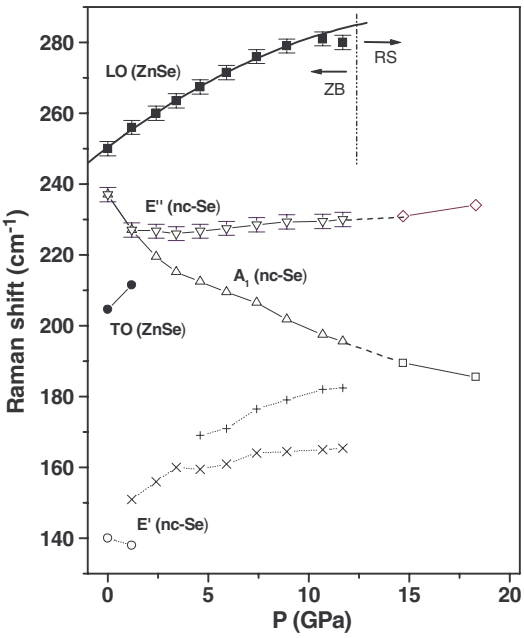

Figure 9. Raman frequency of ZnSe (full symbols) and bulk-Se (empty symbols) modes of the annealed sample (ta-MA-ZnSe) as a function of pressure. The solid line represents the best fitting reached using a second-order polynomial function. Representative error bars are shown for two Raman lines.

(This figure is in colour only in the electronic version)

mechanical deformations, no anomalies were observed for the LO-ZnSe mode with pressure. From these observations several conclusions can be made about the changes of MA-ZnSe physical properties due to thermal annealing. The values of the phase transition pressures of both ZnSe and Se phases can be recovered to those of bulk samples. Furthermore, the non-reacted Se can be manipulated (from nanometric to bulk form) by sample annealing. These characteristics are very promising for technological and scientific points of view, since simple thermal treatments may be able to define the thermodynamic and structural behaviour of the as-milled samples.

The Raman results reinforce the previous speculations about the non-reacted Se of the as-milled sample, which propose its dispersion in the interfacial regions of ZnSe nanocrystals, and showed that the dispersed Se particles are in the nanocrystalline form under high-pressure conditions. However, the situation at ambient conditions remains undefined. Both amorphous and crystalline Se are mainly composed of Se chains, i.e. they have practically the same Raman spectra. In addition, photo- and pressure-induced crystallization of Se has been already reported, which do not allow one to affirm in which state the non-reacted Se is at ambient conditions.

4. Conclusions

Structural and vibrational studies of the MA-ZnSe sample submitted to high-pressure conditions were done and the main conclusions were are follows.

The EXAFS measurements of the MA-ZnSe alloy as a function of pressure suggest important influences of the sample preparation method (known to induce particle size reduction) on the semiconductor–metal transition pressure and on the compressibility as compared with bulk ZnSe. For the MA-ZnSe sample the transition pressure increased while the compressibility decreased.

The Raman results showed that non-reacted Se found in the as-milled sample is in nanocrystalline form under high-pressure conditions. They also showed that the LO-ZnSe

mode of MA-ZnSe is less dispersive than that of the bulk, but after annealing the mechanically alloyed sample showed values comparable to those of bulk samples, even in the second-order polynomial approximation.

The values of the phase-transition pressures of both ZnSe and Se phases observed for the mechanically alloyed sample, as well as the dimensional scale of them (nanometric or bulk form), can be manipulated by thermal annealing processing.

Acknowledgments

We wish to thank the Brazilian agencies (CAPES and CNPq) for financial support. We are also indebted to J C Chervin and B Canny for their helpful technical support in the Raman measurements under pressure.

References

[1] Leppert V J, Mahamuni S, Kumbhojkar N R and Risbud S H 1989 *Mater. Sci. Eng.* B **52** 89
[2] Gleiter H 1989 *Prog. Mater. Sci.* **33** 223
[3] Zhu X, Birringer R, Herr U and Gleiter H 1987 *Phys. Rev.* B **35** 9085
[4] Nelmes R J and McManhon M I 1998 *Semiconductor and Semimetals* vol 54, ed T Suzuki, P Willian and R K Willardson (New York: Academic) and references therein
[5] Côté M, Zakharov O, Rubio A and Cohen M L 1997 *Phys. Rev.* B **55** 13025
[6] Qteish A and Munoz A 2000 *J. Phys.: Condens. Matter* **12** 1705
[7] Pellicer-Porres J, Segura A, Muñoz V, Zuñiga J, Itié J P, Polian A and Munsch P 2001 *Phys. Rev.* B **65** 12109
[8] Kusaba K and Kikegawa T 2002 *J. Phys. Chem. Solids* **63** 651
[9] Greene R G, Luo H and Ruoff A L 1995 *J. Phys. Solids* **56** 521
[10] de Lima J C, dos Santos V H F and Grandi T A 1999 *Nanostruct. Mater.* **11** 51
[11] Machado K D, de Lima J C, Campos C E M, Grandi T A and Gasperini A A M 2003 *Solid State Commun.* **127** 477
[12] Campos C E M, de Lima J C, Grandi T A and Machado K D 2004 *Vib. Spectrosc.* **36** 117
[13] Rietveld H M 1969 *J. Appl. Crystallogr.* **2** 65
[14] Strnad Z 1986 *Glass–Ceramic Materials* (Amsterdam: Elsevier) p 161
[15] Michalowicz A 1997 *J. Phys. Coll.* IV **7** C2 235 and XAFS software catalog on the ESRF web site: http://www.esrf.fr/computing/scientific/exafs/links.html
[16] Hasnain S S (ed) 1991 Report on the international workshops on standards and criteria in XAFS *X-ray Absorption Fine Structure: Proc. 6th Int. Conf. on X-ray Absorption Fine Structures* (New York: Ellis Horwood) p 752 and last S&C reports on the IXS web site (07/2000) http://ixs.iit.edu/subcommittee_reports/sc/
[17] San-Miguel A, Polian A, Gauthier M and Itié J P 1993 *Phys. Rev.* B **48** 8683
[18] Sainctavit P, Itié J P, Polian A and San-Miguel A 1993 *Japan. J. Appl. Phys.* **32** 44
[19] Besson J M, Itié J P, Polian A, Weill G, Mansot J L and Gonzalez J 1991 *Phys. Rev.* B **44** 4212
[20] Itié J P, Polian A, Jauberthie-Carillon C, Dartyge E, Fontaine A, Tolentino H and Tourillon T 1989 *Phys. Rev.* B **40** 9709
[21] Perlin P, Jauberthie-Carillon C, San-Miguel A, Gzegory I and Polian A 1992 *Phys. Rev.* B **45** 83
[22] *ICSD—Inorganic Crystal Structure Database* 1995 Gmchin-Institute fur Anorganishe Chemie and Fachinformationszentrum FIZ
[23] Tranquada J M, Ingalls R and Crozier E D 1984 *EXAFS and Near Edge Structure III* ed K O Hodgson, B Hedman and J E Penner-Hahn (Berlin: Springer) p 374
[24] Murnaghan F D 1944 *Proc. Natl Acad. Sci. USA* **30** 244
[25] Gangadharan R, Jayalakshimi V, Kalaiselvi J, Mohan S, Murugan R and Palanivel B 2003 *J. Alloys Compounds* **359** 22
[26] Cohen M 1985 *Phys. Rev.* B **32** 7988
[27] Al-Douri Y, Abid H and Aourag H 2003 *Physica* B **322** 179
[28] Bandyopadhyay A K and Ming L C 1996 *Phys. Rev.* B **54** 12049
[29] Liu H, Jin C and Zhao Y 2002 *Physica* B **315** 210
[30] McMahon M I, Hejny C, Loveday J S, Lundegaard L F and Hanfland M 2004 *Phys. Rev.* B **70** 054101
[31] Grandi T A, dos Santos V H and de Lima J C 1999 *Solid State Commun.* **112** 359